Available online at www.sciencedirect.com
ScienceDirect
Ceramics International 40 (2014) 643–649
CERAMICS INTERNATIONAL
www.elsevier.com/locate/ceramint

Synthesis and characterization of planar heterojunction hybrid polymer solar cells based on copper pthalocyanine (CuPc) and titanium dioxide

Sawanta S. Mali[a,b], Hyungjin Kim[b], Jin Hyeok Kim[c], Pramod S. Patil[a,c], Chang Kook Hong[b,*]

[a]Department of Physics, Shivaji University, Kolhapur 41004, India
[b]Advanced Chemical Engineering Department, Chonnam national University, Gwangju 500-757, South Korea
[c]Department of Materials Science, Chonnam National University, Gwangju, 500-757, South Korea

Received 1 May 2013; received in revised form 25 May 2013; accepted 14 June 2013
Available online 20 June 2013

Abstract

We report planar heterojunction solar cell obtained by chemical vapor deposition (CVD) and hydrothermal technique. Copper phthalocyanine (CuPc) and titanium oxide (TiO_2) were used as donor and acceptor materials respectively. The nanomorphologies like nanocorals, nanorods and nanoflowers were synthesized by the hydrothermal route and CuPc was deposited by CVD. The optical and compositional properties of TiO_2/CuPc films were investigated by using UV–vis spectroscopy and X-ray photoelectron spectroscopy (XPS). Finally TiO_2/CuPc devices were tested for their *J–V* properties. This approach would be quite useful for the fabrication of hybrid solar cells. The TiO_2/CuPc device shows maximum photoconversion efficiency (η%) 0.41% for TiO_2 nanoflower like morphology.

Keywords: TiO_2/CuPc planar heterojunction solar cells; XPS; 0.41% conversion efficiency

1. Introduction

Recently, polymer solar cell (PSCs) based on conducting polymers (CPs) and fullerene (C_{60}) have been widely investigated due to their advantages of low-cost, light weight, easy fabrication, and possibility to fabricate flexible devices which is not feasible with inorganic materials. PSCs are mainly classified into two categories: (i) Planar heterojunction and (ii) Bulk Heterojunction.

The planar heterojunction organic polymer bilayer solar cell was invented by Tang in the mid-1980s and achieved power conversion efficiency (PCE) of about 1% [1]. In PSC usually light is absorbed in the donor materials like Poly(3-hexylthiophene-2,5-diyl) (P3HT), Poly[2-methoxy-5-(3′,7′-dimethyloctyloxy)-1,4-phenylenevinylene](MDMO:PPV), Poly[[9-(1-octylnonyl)-9H-carbazole-2,7-diyl]-2,5-thiophenediyl-2,1,3-benzothiadiazole-4,7-diyl-2,5-thiophenediyl] (PCDTBT) or small molecule such as copper phthalocyanine (CuPc), zinc phthalocyanine (ZnPc), aluminum phthalocyanine (AlPc). In bilayer devices, the photogenerated singlet exciton could diffuse within donor towards the planar interface to the second material, the acceptor, which is usually chosen to be strongly electronegative (fullerene or Phenyl-C_{61}-butyric acid methyl ester ($PC_{61}BM$)) materials. The acceptor material provides the energy needed for the singlet exciton to be separated, as the electron can go to a state of much lower energy within the acceptor. This charge transfer dissociates the exciton, the electron moves to the acceptor material, whereas the hole remains on the donor. A prominent example for an electron acceptor material is the buckminsterfullerene (C_{60}) and its derivatives like $PC_{71}BM$.

The planar heterojunction polymer solar cell consists of a thin active layer sandwiched between two electrodes. Typically a transparent indium tin oxide (ITO) coated glass substrate and relatively low work function metal cathode aluminum (Al) were used as two electrodes. The active layer is made up of two light-absorbing semiconducting polymers, one with an electron-donating character (donor: D) and the other with an

*Corresponding author. Tel.: +82 62 530 0635.
E-mail addresses: sawantamali@yahoo.co.in (S.S. Mali), hongck@chonnam.ac.kr (C. Kook Hong).

0272-8842/$ - see front matter
http://dx.doi.org/10.1016/j.ceramint.2013.06.050

electron-accepting character (acceptor: A). These semiconductors could either be deposited as two distinct layers where the donor–acceptor interface resides only between the two layers (bilayer), or be blended as an almost homogeneous mix where interfacial interaction between donor and acceptor exists throughout the blended bulk layer (bulk heterojunction (BHJ)). Operation processes of an organic photovoltaic device on the molecular level consist of three consecutive fundamental steps: (1) absorption of light, (2) creation of separate charges at the donor–acceptor interface, and (3) selective transport of charges through the bulk of the device to the appropriate collecting electrodes [1–2].

These photovoltaic devices predominantly use the fullerene derivatives like [C_{60}]PCBM and [C_{70}]PCBM as the electron accepting component and P3HT, MDMO:PPV, PCDTBT, MEH-PPV (poly-[1-methoxy-4-(2-ethylhexyl)-2,5-phenylene-vinylene]) and some low band gap polymers are most extensively used as a electron donor. However, there are some drawbacks of PCBM for application in PSCs, including weak absorption in the visible region and the possibility of phase separation from the polymer donor. On the other hand, due to its high cost P3HT and other electron donor materials will increase the cost of the device. Therefore, non-fullerene based hybrid devices [3–4] and all PSCs in which a metal pthalocyanines (MPcs) as a donor have attracted interest recently [5–11].

Recently, organo-metallics, in particular small molecular polymers like metal-substituted phthalocyanines (MPcs) are planar conjugated aromatic macrocycles forming molecular crystals with conductivities ranging from 10^{-12} up to 10^{-4} Sm^2 and it shows a rich absorption spectrum in the ultraviolet and visible ranges. These MPcs like CuPc, ZnPc and AlPc are most studied and well-suited as a donor material. Since, they show a rich absorption spectrum in the ultraviolet and visible ranges. CuPc having highest occupied molecular orbital (HOMO) and lowest unoccupied molecular orbital (LUMO) 5.2 and 3.3 eV respectively and is widely used in PSC application [12–18] as donor material.

On the other hand, non-fullerene acceptors for organic photovoltaics become opened a new way to low develop photovoltaic technology. Number of non-fullerene acceptors like (i) Rylene diimide-based acceptors materials e.g. trans-perylene tetracarboxylic derivative [19], Oligothiophene-S, S-dioxide based acceptors e.g. thiophenyl-S,S-dioxide-based oligomer [20], Cyano-PPV and other cyano-based acceptors e. g. cyano-poly(phenylene vinylene) [21], Pigments and dyes e. g. tricyclic sodium 2-(6-oxido-3-oxo-3H-xanthen-9-yl)benzoate component [22], 2-Vinyl-4,5-dicyanoimidazole (Vinazene) based acceptors [23], Diketopyrrolopyrrole based acceptors e. g. dodecylsubstituted Diketopyrrolopyrrole [24] and other polymers like Poly[(1,4-divinylenephenylene)(2,4,6-triisopropylphenylborane)] [25]. P. Sonar et al. [26] was best reviewed the progress in the synthesis, characterization and implementation of the various classes of non-fullerene based n-type organic acceptors for photovoltaic applications.

Very few reports are available based on inorganic materials like n-type titanium oxide (TiO_2) as an acceptor for planar heterojunction solar cell applications [27–31]. TiO_2 is a versatile material and has been investigated considerably due to its unique photoelectrochemical properties and optoelectronic such as high refractive index (2.488 anatase, 2.609 rutile), high dielectric constant (ε_a=86, ε_c=170), excellent optical transmittance in the visible and near-IR region. The nanoparticulate TiO_2 has been widely used as a promising electron-transport material in dye-sensitized solar cells (DSSCs) [32] and quantum dot sensitized solar cells (QDSSCs) [33] application. Therefore, in the present investigation TiO_2 and CuPc have been selected as acceptor and donor materials respectively for the hybrid polymer solar cells (HPSC). The different nanostructures of TiO_2 like nanocoral, nanorods and nanoflowers were deposited by hydrothermal technique and CuPc layer was deposited by vacuum evaporation. Finally the current voltage (J–V) properties of the TiO_2/CuPc based device were recorded using Al contact as counter electrode.

2. Experimental

2.1. Chemicals and materials:

The conducting Fluorine doped tin oxide (FTO) coated glass substrates were purchased from Kintech Co. Hong Kong (FTO, sheet resistance 15 $\Omega\,cm^{-2}$, transmittance 90%). Prior to the deposition, FTO substrates were successively cleaned in ultrasonic, detergent, acetone, ethanol and 2-isopropanol and dried in oven at 70 °C.

2.2. Methods

The different morphology like nanocoral (TNC), nanorod (TNR) and nanoflowers (TNF) of TiO_2 were synthesized by hydrothermal process as per our previous report [34–39]. Briefly TNC samples were deposited using $TiCl_4$ precursor at 120 °C while TNR and TNF samples were deposited using titanium tetra isopropoxide (TTIP) precursor at 180 °C. Deposited TiO_2 samples were dried at 60 °C in oven and used for further CuPc deposition. The CuPc evaporation process is performed within a vacuum chamber under 10^{-5} mbar with deposition rate of 0.3–0.5 Å/s. The electric current was adjusted slowly from 0.0 up to 2.2 A (10 V) to allow heating the molybdenum (Mo) boat, then the CuPc starts evaporating and films of ~20 nm thickness were deposited at room temperature [40]. Al-contact was taken by evaporation of Al–Metal foil as the cathode. The active area of the device was 0.5 cm × 0.5 cm.

2.3. Characterizations

The optical absorption spectra were recorded by using UV–vis spectrophotometer (Shimadzu, model UV-1800, Japan) in the wavelength range of 300–1100 nm with 0.01 nm resolution. The elemental composition of the TiO_2/CuPc sample was analyzed using an x-ray photoelectron spectrometer (XPS) (Thermo K-Alpha) with multi-channel detector, which can suffer high photonic energies from 0.1 to 3 keV.

2.4. J–V measurements

The current density–voltage (*J–V*) performance of the devices were tested by using 2420 source meter under illuminated with AM1.5 from solar simulator 100 mW/cm^2 (Photo Emission Tech. INC Camarillo, CA 9312, USA Solar Simulator, Model # CT80AAA, Serial # 1038). The illumination intensity was calibrated with a standard silicon photovoltaic traced to the National Renewable Energy Laboratory (NREL). The following cell configurations were used to record *J–V* plots:

$$\text{Glass/FTO/TNC/CuPc/Al} \quad (\text{Device} - 1) \tag{1}$$

$$\text{Glass/ FTO/TNC/CuPc/Al} \quad (\text{Device} - 2) \tag{2}$$

$$\text{Glass/ FTO/TNC/CuPc/Al} \quad (\text{Device} - 3) \tag{3}$$

All the measurements were carried out at room temperature.

3. Results and discussion

3.1. Schematic energy level diagram of TiO_2/CuPc planar heterojunction

The schematic diagram with energy levels of TiO_2/CuPc planar heterojunction hybrid polymer solar cell is shown in Fig. 1. The device mechanism is described as below. The excitons are generated in the charge generation material (CuPc) upon exposure to light and dissociated into free holes and electrons at the interface between the electron donor (CuPc) and electron acceptor (TiO_2). Then the free holes and electrons migrate through their respective transportation channels to the corresponding electrodes. The TiO_2 nanostructures can enormously increase the contact areas between CuPc and TiO_2, which offers many more sites for the excitons.

As can be found from the energy levels shown in Fig. 1, the HOMO of CuPc and TiO_2 (conduction band) are 5.2 eV and 7.4 eV, respectively. The barrier energy between them forbids holes running into TiO_2 effectively. The energy difference between the LUMO of CuPc (3.5 eV) and LUMO TiO_2 (4.2 eV) does the same thing on electrons. The slight difference in energy bands of CuPc and TiO_2 with their respective contact electrodes (Al for CuPc, and FTO for TiO_2) is favorable for photogenerated charge carriers transferring from CuPc and TiO_2 to Al and FTO electrodes, respectively.

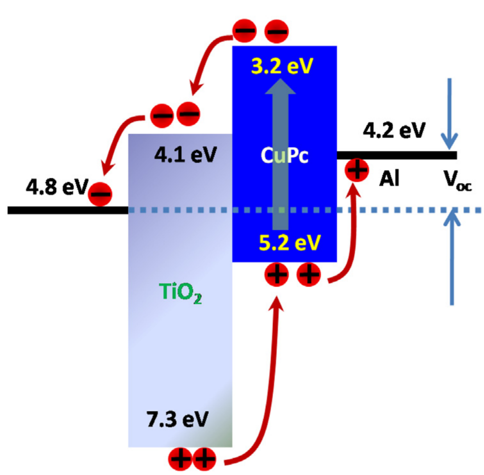

Fig. 1. Schematic gnergy level diagram of the TiO_2/CuPc device. Energy level values are given in eV with respect to the vacuum level.

3.2. UV–vis spectroscopy

Fig. 2 shows the UV–vis absorption spectra of TNC/CuPc, TNR/CuPc and TNF/CuP thin film samples. All the samples show, the Davydov splitting (ΔQ) due to first and second π–π^* transition at 770 and 552 nm respectively [41,42]. Also same films are showing sharp peak at 380 nm is due to TiO_2 band edge absorption. The TNF/CuPc sample shows more absorption compared to both, this is due to effective light scattering in the nanoflower morphology of the TiO_2.

3.3. X-ray photoelectron spectroscopy (XPS) of TNF/CuPc

Fig. 3(a) shows the XPS survey scanning spectrum recorded at the raw surface of the TNF/CuPc device. There were eight relatively strong peaks in the XPS whole scanning spectrum. The peaks located at about 937, 402 and 290 eV correspond to the electron states of Cu(2p), N 1s and C 1s in the CuPc molecule, respectively. The Ti(2p) and O 1s peak is approximately located at 459 eV and 534 eV respectively [34]. Fig. 3 (b) shows the core level spectra of Cu(2p), with two peaks at 935.55 (Cu($2p_{3/2}$))and 955.46 eV (Cu($2p_{1/2}$)), indicating a 19.91 eV split of Cu(I), which is consistent with the standard separation of 19.91 eV. Theoretically, as the interface of CuPc and TNF films is approached, the intensity of Cu 2p peak should reduce because of the decrement of copper atomic concentration, but in fact, the Cu(2p) peak almost stays the

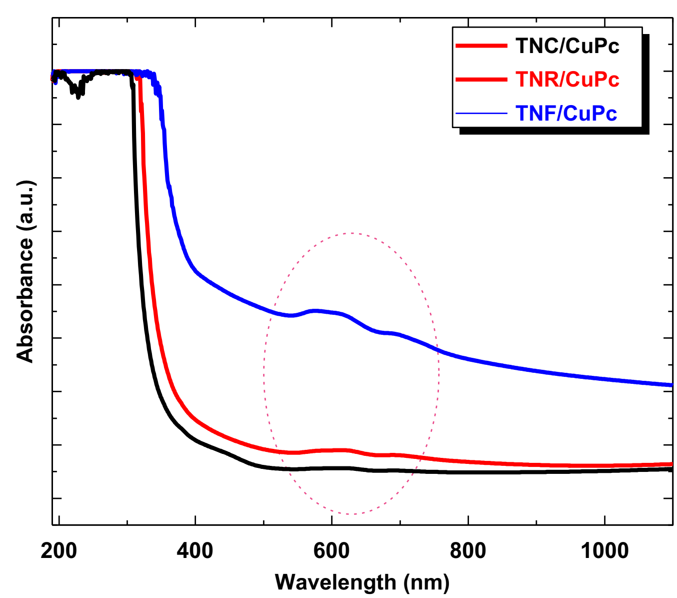

Fig. 2. Optical absorption spectra of TNC/CuPC, TNR/CuPc and TNF/CuPc samples.

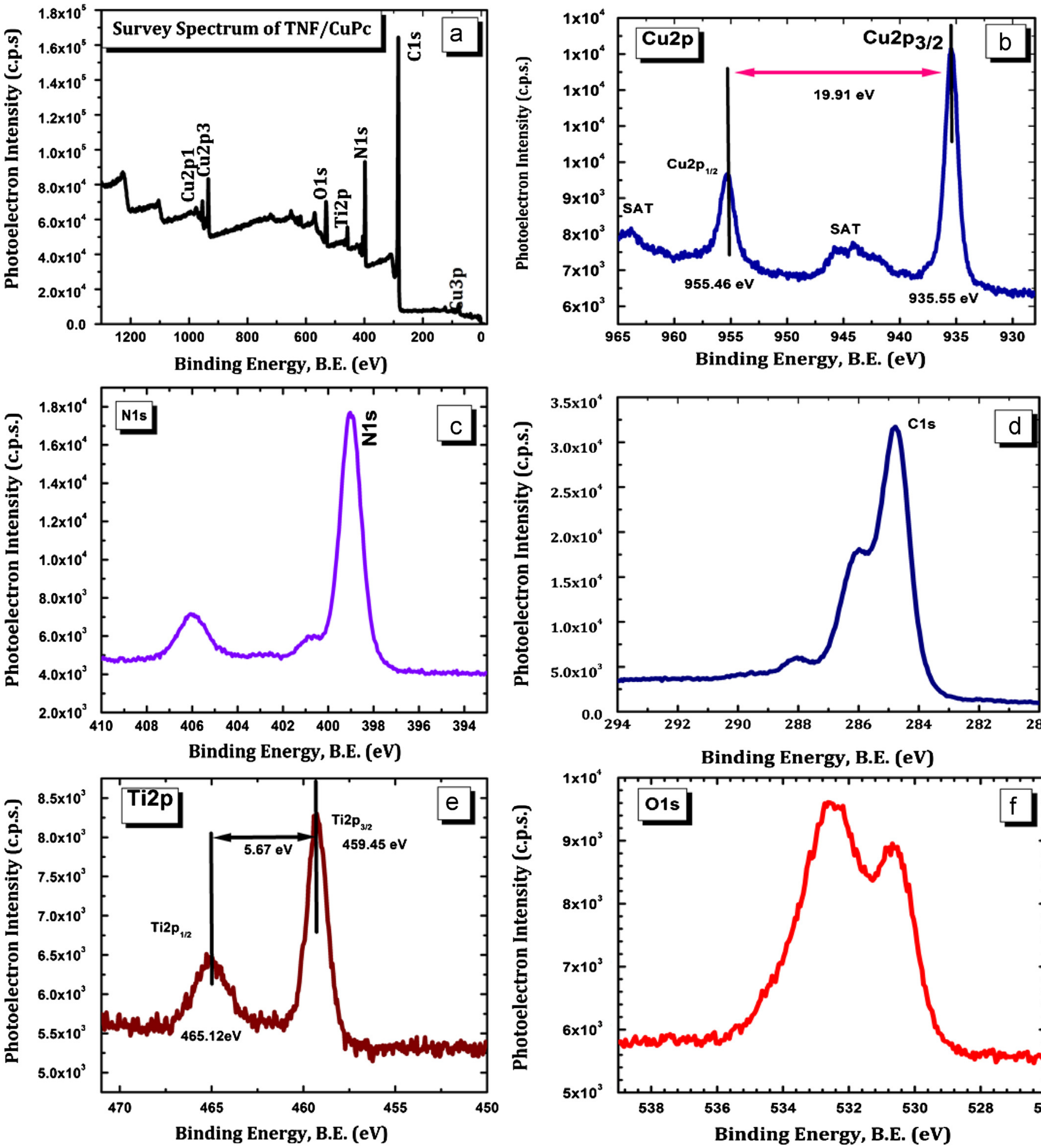

Fig. 3. The XPS spectra of TNF/CuPc sample (a) representative XPS survey spectrum of TNF/CuPc sample (b) core-levels of Cu($2p_{3/2}$) and Cu($2p_{1/2}$), (c) curve fit of N1s peak, (d) Curve fit of C1s peak, (e) core-level lines of Ti ($2p_{3/2}$) and Ti ($2p_{1/2}$) and (f) core-level lines of O1s (SAT—satellite peak).

same. This may originate from the copper atoms detached themselves from the chemical bonds in CuPc molecules diffused into the interface of TNF/CuPc (Fig. 3(b)). For the C(1s) and N(1s) spectra, the peak area reduces and the peak positions shift towards higher binding energy. The alteration of peak positions of C(1s) and N(1s) may be due to the effect of oxygen originated from the TiO_2 nanoflower film and absorbed O_2 and H_2O [43,44].

As the interface of TNF/CuPc interface come in to picture, the concentration of oxygen mainly originating from the TiO_2 film increases, and the interaction of oxygen with carbon and nitrogen atoms strengthens, which causes the C 1s and N 1s peaks shift towards higher binding energy (Fig. 3(c and d)). Moreover, from Fig. 3(b) it is clearly seen that the satellite peak at 289.1 eV is intense, which further indicates that more oxygen is present close to the TiO_2 interface. The TNF/CuPc device exhibits Ti2p photoelectron peaks with a slight asymmetry at the lower binding energy side of the peaks. Further, the spectrum of the film does not show a strong satellite at 14 eV from $Ti(2p_{3/2})$ peak which is characteristic of TiO_2. The position of the $Ti(2p_{3/2})$ peak at 459.1 eV and the shoulder at 458.0 eV indicate the presence of Ti^{3+} and Ti^{4+} oxidation states. The core-levels of O 1s spectrum shift towards higher binding energy, which similar to that of C 1s and N 1s spectra, but the peak area of O 1s spectrum is increases (Fig. 3(f)). The O1s spectrum shows a main peak at 530.6 eV and a shoulder at ~532.1 eV. The peak at 530.6 eV is assigned to oxygen bound to tetravalent Ti ions. The observed peak position, the doublet separation between the $2p_{1/2}$ and $2p_{3/2}$ peaks of ~5.67 eV and the strong satellite at ~14 eV from the main peak are the characteristic of TiO_2. The shape and binding energy of the O1s peak are similar to that of as deposited layers and could also be denconvoluted in the same two components.

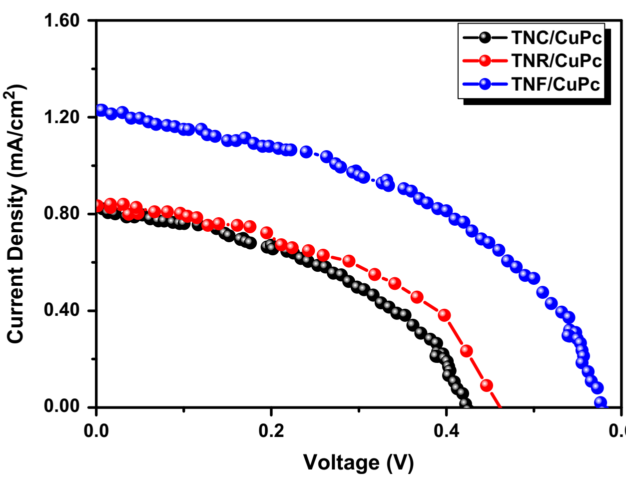

Fig. 4. *J–V* characteristics of TiO2/CuPc; TNC/CuPc, TNR/CuPc and TNF/CuPc devices.

3.4. *J–V* measurements of TiO_2/CuPc devices

Fig. 4 shows the *J–V* plots of both the TiO_2/CuPc devices. The average photovoltaic data were summarized in Table 1. The TNC/CuPc sample shows $J_{sc}=0.834$ mA/cm^2, $V_{oc}=0.419$ V with conversion efficiency 0.18%. The TNR/CuPc device shows 0.20% solar energy conversion efficiency. The highest conversion efficiency of TNF/CuPc device shows 0.41%. The Table 1 indicates that the TNF/CuPc device exhibits higher conversion efficiency than TNC/CuPc and TNR/CuPc devices. This enhancement is due to the large contact area between TNF and CuPc facilitated the photoinduced charge transfer from CuPc to TiO_2, which together with 1.182 mA/cm^2 current density. The directional alignment of TiO_2 nanowires was favorable to the following charge separation and transport processes. Photoreceptors from donor–acceptor with high photosensitivities owing to the photoinduced charge transfer between the donor and the acceptor. The photographs of fabricated TiO^2/CuPc devices are shown in Fig. 5.

The one-dimensional (1D) and well-ordered structure of TiO_2 nanoflowers arrays can act as an efficient transport channel. With the help of the TiO_2 nanoflowers, the collection efficiency of electrons is greatly enhanced, leading to an evident increase of photocurrent. However, the large donor/acceptor contact area improves the probability to form traps or recombination centers at the interface. When the devices are illuminated, traps will be gradually filled before the photocurrent reaches a steady state. Thus the carriers collected by

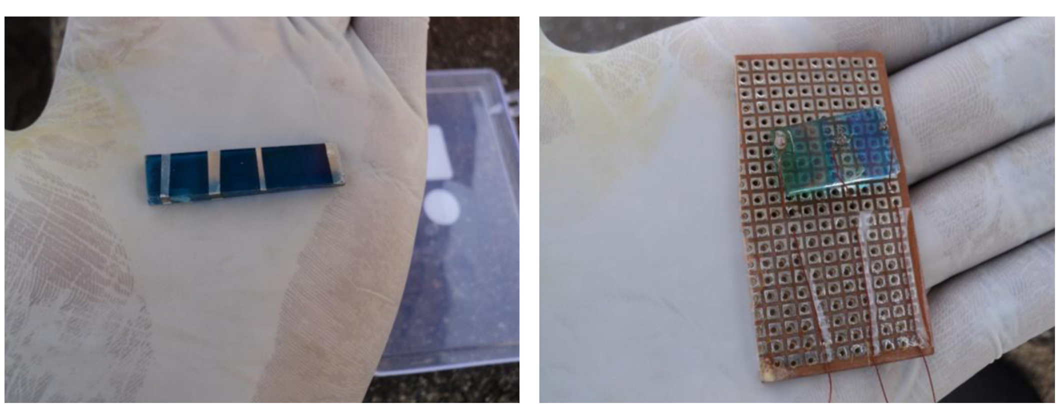

Fig. 5. Photographs of fabricated TiO_2/CuPc devices.

Table 1
Solar cell parameters of TiO_2/CuPc devices.

Sample	*J*sc (mA/cm^2)	*V*oc (V)	*J*max (mA/cm^2)	*V*max (V)	*R*s (Ω)	*R*sh (kΩ)	Ideality factor (n_d)	*FF*	(η) %
Device-1	0.834	0.419	0.623	0.407	134	1.035	2.12	0.49	0.18
Device-2	0.865	0.432	0.711	0.434	167	1.457	2.36	0.53	0.20
Device-3	1.182	0.591	0.910	0.493	123	1.224	2.35	0.58	0.41

electrodes will increase step by step. As the devices are switched to dark, not only the non-equilibrium electrons in conduction band of TiO_2 but also the electrons released from traps are recombined with holes. For those deep level traps, the thermal excitation of trapped electrons to conduction band is difficult so that they can be treated as recombination centers. Then the photocurrent will reduce slowly depending upon these releasing courses. A similar process happens in the p-type semiconductor of CuPc.

4. Conclusions

In conclusion, hybrid polymer solar cells (HPSC) based on TiO_2/CuPc planar heterojunction were successfully fabricated and tested. Our results revealed that the planar heterojunction device based on TNF/CuPc sample shows PCE (η)=0.41% (Jsc=1.182 mA/cm^2, Voc=0.591 V). This value is higher 44% and 63% higher than that of TNC/CuPc and TNR/CuPc based devices respectively. This enhancement is due to the large contact area between TNF and CuPc facilitated the photoinduced charge transfer from CuPc to TiO_2, which together with the directional alignment of TiO_2 nanowires was favorable to the following charge separation and transport processes. Photoreceptors from donor–acceptor nanocomposites with high photosensitivities owing to the photoinduced charge transfer between the donor and the acceptor.

Acknowledgment

This work was supported by the Priority Research Centers Program through the National Research Foundation of Korea (NRF) funded by the Ministry of Education, Science and Technology (2009–0094055). This work is partially supported by the Human Resource Development of the Korea Institute of Energy technology Evaluation and Planning (KETEP) Grant funded by the Korea Government Ministry of knowledge Economy (No. 20124010203180).

References

[1] G. Li, V. Shrotriya, J.S. Huang, Y. Yao, T. Moriarty, K. Emery, Y. Yang, High-efficiency solution processable polymer photovoltaic cells by self-organization of polymer blends, Nature Materials 4 (2005) 864.
[2] N.S. Sariciftci, L. Smilowitz, A.J. Heeger, F. Wudl, Photoinduced electron transfer from a conducting polymer to buckminsterfullerene, Science 258 (1992) 1474.
[3] F.C. Krebs, Air stable polymer photovoltaics based on a process free from vacuum steps and fullerenes, Solar Energy Materials and Solar Cells 92 (2008) 715.
[4] M.S. White, D.C. Olson, S.E. Shaheen, N. Kopidakis, D.S. Ginley, Inverted bulk-heterojunction organic photovoltaic device using a solution-derived ZnO underlayer, Applied Physics Letters 89 (2006) 143517.
[5] J.J.M. Halls, C.A. Walsh, N.C. Greenham, E.A. Marseglia, R.H. Friend, S.C. Moratti, A.B. Holmes, Efficient photodiodes from interpenetrating polymer networks, Nature 376 (1995) 498.
[6] A.C. Arias, J.D. MacKenzie, R. Stevenson, J.J.M. Halls, M. Inbasekaran, E.P. Woo, D. Richards, R.H. Friend, Photovoltaic performance and morphology of polyfluorene blends: a combined microscopic and photovoltaic investigation, Macromolecules 34 (2001) 6005.
[7] Y. Kim, S. Cook, S.A. Choulis, J. Nelson, J.R. Durrant, D.D.C. Bradley, Organic photovoltaic devices based on blends of regioregular poly (3-hexylthiophene) and poly(9,9-dioctylfluorene-co-benzothiadiazole), Chemistry of Materials 16 (2004) 4812.
[8] S.C. Veenstra, W.J.H. Verhees, J.M. Kroon, M.M. Koetse, J. Sweelssen, J.J.A.M. Bastiaansen, H.F.M. Schoo, X. Yang, A. Alexeev, J. Loos, U.S. Schubert, M.M. Wienk, Photovoltaic properties of a conjugated polymer blend of MDMO−PPV and PCNEPV, Chemistry of Materials 16 (2004) 2503.
[9] A.J. Breeze, Z. Schlesinger, S.A. Carter, H. Tillmann, H.H. Horhold, Improving power efficiencies in polymer–polymer blend photovoltaics, Solar Energy Materials and Solar Cells 83 (2004) 263.
[10] T. Kietzke, H.H. Horhold, D. Neher, Efficient polymer solar cells based on M3EH−PPV, Chemistry of Materials 17 (2005) 6532.
[11] Z. Tan, E. Zhou, X. Zhan, X. Wang, Y. Li, S. Barlow, S.R. Marder, Efficient all-polymer solar cells based on blend of tris(thienylenevinylene)-substituted polythiophene and poly[perylene diimide-alt-bis(dithienothiophene)], Applied Physics Letters 93 (2008) 073309.
[12] P. Peumans, S.R. Forrest, Very-high-efficiency double-heterostructure copper phthalocyanine/C_{60} photovoltaic cells, Applied Physics Letters 79 (2001) 126.
[13] P. Peumans, V. Bulovic, S.R. Forrest, Efficient photon harvesting at high optical intensities in ultrathin organic double-heterostructure photovoltaic diodes, Applied Physics Letters 76 (2000) 2650.
[14] A. Yakimov, S.R. Forrest, High photovoltage multiple-heterojunction organic solar cells incorporating interfacial metallic nanoclusters, Applied Physics Letters 80 (2002) 1667.
[15] J. Xue, Soichi Uchida, Barry P. Rand, Stephen R. Forrest, 4.2% efficient organic photovoltaic cells with low series resistances, Applied Physics Letters 84 (2004) 3013.
[16] Soichi Uchida, Jiangeng Xue, Barry P. Rand, Stephen R. Forrest, Organic small molecule solar cells with a homogeneously mixed copper phthalocyanine: C60 active layer, Applied Physics Letters 84 (2004) 4218.
[17] L.G.D. Arco, Y. Zhang, C.W. Schlenker, K. Ryu, M.E. Thompson, C. Zhou, Continuous, highly flexible, and transparent graphene films by chemical vapor deposition for organic photovoltaics, ACS Nano 4 (2010) 2865.
[18] H. Xi, Z. Wei, Z. Duan, W. Xu, D. Zhu, Facile method for fabrication of nanostructured CuPC thin films to enhance photocurrent generation, Journal of Physical Chemistry C 112 (2008) 19934.
[19] C.W. Tang, Two-layer organic photovoltaic cell, Applied Physics Letters 48 (1986) 183.
[20] N. Camaioni, G. Ridolfi, V. Fattori, L. Favaretto, G. Barbarella, Oligothiophene-S,S-dioxides as a class of electron-acceptor materials for organic photovoltaics, Applied Physics Letters 84 (2004) 1901.
[21] M. Granstrom, K. Petritsch, A.C. Arias, A. Lux, M.R. Andersson, R.H. Friend, Laminated fabrication of polymeric photovoltaic diodes, Nature 395 (1998) 257.
[22] B. Pradhan, A.J. Pal, Organic heterojunction photovoltaic cells: role of functional groups in electron acceptor materials, Solar Energy Materials and Solar Cells 81 (2004) 469.
[23] T. Kietzke, R.Y.C. Shin, D.A.M. Egbe, Z.K. Chen, A. Sellinger, Effect of annealing on the characteristics of organic solar cells: polymer blends with a 2-vinyl-4,5-dicyanoimidazole derivative, Macromolecules 40 (2007) 4424.
[24] P. Sonar, G.M. Ng, T.T. Lin, A. Dodabalapur, Z.K. Chen, Solution processable low bandgap diketopyrrolopyrrole (DPP) based derivatives: novel acceptors for organic solar cells, Journal of Materials Chemistry 20 (2010) 3626.
[25] S. Cataldo, S. Fabiano, F. Ferrante, F. Previti, S. Patane, B. Pignataro, Polymer brushes via controlled, surface-initiated atom transfer radical polymerization (ATRP) from graphene oxide, Macromolecular Rapid Communications 31 (2010) 281.
[26] P. Sonar, J. Pui, F. Lim, K.L. Chan, Organic non-fullerene acceptors for organic photovoltaics, Energy and Environmental Science 4 (2011) 1558.
[27] Liang Shen, G. Zhu, W. Guo, C. Tao, X. Zhang, C. Liu, W. Chen, S. Ruan, Z. Zhong, Performance improvement of TiO_2/P3HT solar cells using CuPc as a sensitizer, Applied Physics Letters 92 (2008) 073307.

[28] Raj Kumar, G.D. Sharma, M.S. Roy, Hybrid nano-crystalline TiO_2 solar cell with copper phthalocyanine as sensitizer and hole transporter, Indian Journal of Pure and Applied Physics 49 (2011) 557.
[29] M. Ouyang, R. Bai, L. Yang, Q. Chen, Y. Han, M. Wang, Y. Yang, H. Chen, High photoconductive vertically oriented TiO_2 nanotube arrays and their composites with copper phthalocyanine, Journal of Physical Chemistry C 112 (2008) 2343.
[30] Y. Wang, Y. Ye, K. Wu, Adsorption and assembly of copper phthalocyanine on cross-linked $TiO_2(110)$-(1×2) and $TiO_2(210)$, Journal of Physical Chemistry B 110 (2006) 17960.
[31] Mingyi Zhang, Changlu Shao, Zengcai Guo, Zhenyi Zhang, Jingbo Mu, Tieping Cao, Yichun Liu, , Hierarchical nanostructures of copper(II) phthalocyanine on electrospun TiO_2 nanofibers: controllable solvothermal-fabrication and enhanced visible photocatalytic properties, ACS Applied Materials and Interfaces 3 (2011) 369.
[32] S.S. Mali, C.A. Betty, P.N. Bhosale, P.S. Shinde, M.R. Pramod, S.R. Jadkar, P.S. Patil, Efficient dye-sensitized solar cells based on hierarchical rutile TiO_2 microspheres, CrystEnggComm 14 (2012) 8156.
[33] S.S. Mali, R.S. Devan, Yuan-Ron Ma, C.A. Betty, P.N. Bhosale, R.P. Panmand, B.B. Kale, S.R. Jadkar, P.S. Patil, J.H. Kim, C. K. Hong, Effective light harvesting in CdS nanoparticle-sensitized rutile TiO_2 microspheres, Electrochimica Acta 90 (2013) 666.
[34] S.S. Mali, P.S. Shinde, C.A. Betty, P.N. Bhosale, W.J. Lee, P.S. Patil, Nanocoral architecture of TiO_2 by hydrothermal process: synthesis and characterization, Applied Surface Science 257 (2011) 9737.
[35] S.S. Mali, S.K. Desai, D.S. Dalavi, C.A. Betty, P.N. Bhosale, P.S. Patil, CdS-sensitized TiO_2 nanocorals: hydrothermal synthesis, characterization, application, Photochemical and Photobiological Sciences 10 (2011) 1652.
[36] S.S. Mali, C.A. Betty, P.N. Bhosale, P.S. Patil, Eosin-Y and N3-Dye sensitized solar cells (DSSCs) based on novel nanocoral TiO_2: a comparative study, Electrochimica Acta 59 (2012) 113.
[37] S.S. Mali, S.K. Desai, S.S. Kalagi, C.A. Betty, P.N. Bhosale, R.S. Devan, Y.R. Ma, P.S. Patil, PbS quantum dot sensitized anatase TiO_2 nanocorals for quantum dot-sensitized solar cell applications, Dalton Transactions 41 (2012) 6130.
[38] S.S. Mali, C.A. Betty, P.N. Bhosale, R.S. Devan, Y.R. Ma, S.S. Kolekar, P.S. Patil, Hydrothermal synthesis of rutile TiO_2 nanoflowers using Brønsted Acidic Ionic Liquid [BAIL]: synthesis, characterization and growth mechanism, CrystEnggComm 14 (2012) 1920.
[39] S.S. Mali, C.A. Betty, P.N. Bhosale, P.S. Patil, Synthesis, characterization of hydrothermally grown MWCNT–TiO_2 photoelectrodes and their visible light absorption properties, ECS Journal of Solid State Science and Technology 1 (2) (2012) M15–M23.
[40] S.S. Mali, D.S. Dalavi, P.N. Bhosale, C.A. Betty, A.K. Chuahan, P.S. Patil, Electro-optical properties of copper phthalocyanines (CuPc) vacuum deposited thin films, RSC Advances 2 (2012) 2100–2104.
[41] E. Jungyoon, S. Kim, E. Lim, K. Lee, D. Cha, B. Friedman, Effects of substrate temperature on copper(II) phthalocyanine thin films, Applied Surface Science 205 (2003) 274.
[42] B.H. Schechtman, W.E. Spicer, Near infrared to vacuum ultraviolet absorption spectra and the optical constants of phthalocyanine and porphyrin films, Journal of Molecular Spectroscopy 33 (1970) 28.
[43] F. Evangelista, V. Carravetta, G. Stefani, B. Jansik, M. Alagia, S. Stranges, A. Ruocco, Electronic structure of copper phthalocyanine: an experimental and theoretical study of occupied and unoccupied levels, Journal of Chemical Physics 126 (2007) 124709.
[44] H. Kato, S. Takemura, S. Kimura, T. Okumura, D. Kobayakawa, Y. Watanabe, T. Sugiyama, T. Hiramatsu, N. Nanba, O. Nishikawa, M. Taniguchi, Nanoscale molecular patterning on artificially fabricated nanoscale structured Al surfaces, Journal of Physics: Conference Series 100 (2008) 052018.